



Fragment antigen binding domains (F_{ab} s) as tools to study assembly-line polyketide synthases

Katarina M. Guzman^a, Chaitan Khosla^{a,b,*}

^a Department of Chemical Engineering, Stanford University, Stanford, CA, 94305, USA

^b Department of Chemistry, Stanford ChEM-H, Stanford University, Stanford, CA, 94305, USA

ARTICLE INFO

Keywords:

Crystallography

Cryo-EM

Polyketide synthases

Fragment antigen binding domains

ABSTRACT

The crystallization of proteins remains a bottleneck in our fundamental understanding of their functions. Therefore, discovering tools that aid crystallization is crucial. In this review, the versatility of fragment-antigen binding domains (F_{ab} s) as protein crystallization chaperones is discussed. F_{ab} s have aided the crystallization of membrane-bound and soluble proteins as well as RNA. The ability to bind three F_{ab} s onto a single protein target has demonstrated their potential for crystallization of challenging proteins. We describe a high-throughput workflow for identifying F_{ab} s to aid the crystallization of a protein of interest (POI) by leveraging phage display technologies and differential scanning fluorimetry (DSF). This workflow has proven to be especially effective in our structural studies of assembly-line polyketide synthases (PKSs), which harbor flexible domains and assume transient conformations. PKSs are of interest to us due to their ability to synthesize an unusually broad range of medically relevant compounds. Despite years of research studying these megasynthases, their overall topology has remained elusive. One F_{ab} in particular, 1B2, has successfully enabled X-ray crystallographic and single particle cryo-electron microscopic (cryoEM) analyses of multiple modules from distinct assembly-line PKSs. Its use has not only facilitated multidomain protein crystallization but has also enhanced particle quality via cryoEM, thereby enabling the visualization of intact PKS modules at near-atomic (3–5 Å) resolution. The identification of PKS-binding F_{ab} s can be expected to continue playing a key role in furthering our knowledge of polyketide biosynthesis on assembly-line PKSs.

1. Introduction

Structural analysis of enzymes is invaluable in understanding their functions and enabling their engineering. However, a major bottleneck exists in obtaining high-quality diffracting protein crystals for structural analysis at atomic resolution. Traditional methods to optimize crystal quality employ cofactors, additives, and seeding to enhance crystal growth or quality. But in the absence of lead crystals, there can be no optimization. Protein crystallization chaperones (CCs) may fill this need by binding to a protein of interest (POI) and increasing their probability of crystallization [1]. One of the first reported instances of CCs dates back to 1987 when an antigen-binding fragment (F_{ab}) complexed with N9 neuraminidase enhanced crystal growth [2]. A F_{ab} is just one of many types of CCs; the list includes scFvs [3], V_HHs [4–6] (or nanobodies [7]), affibodies [8], and DARPins [9] (Fig. 1). Each CC offers unique advantages; moreover they can complement each other based on

differences in their epitope sites (e.g., F_{ab} -DARPin-POI or DARPin-V_HH-POI) [10,11]. Here we focus on applications of F_{ab} s as CCs. We propose a high-throughput workflow for identifying F_{ab} CCs. We also summarize examples of how their deployment to study polyketide synthases (PKSs) could address longstanding questions in biochemical problem areas of interest.

2. Fabs as crystallization chaperones (CCs)

F_{ab} CCs have been useful in a broad range of protein crystallization efforts (Fig. 2) [12–18]. Their ability to increase sample homogeneity [1], improve model-phasing, and mask flexible or charged residues [18, 19] are just a few examples of mechanisms that have led to their adoption as CCs. Additionally, advances in phage display library technologies have increased the probability of obtaining a F_{ab} that complexes tightly with the POI [20,21]. Compared to traditional hybridoma

Peer review under responsibility of KeAi Communications Co., Ltd.

* Corresponding author. Department of Chemical Engineering, Stanford University, Stanford, CA, 94305, USA.

E-mail address: khosla@stanford.edu (C. Khosla).

<https://doi.org/10.1016/j.synbio.2021.12.003>

Received 29 October 2021; Received in revised form 2 December 2021; Accepted 3 December 2021

2405-805X/© 2021 The Authors. Publishing services by Elsevier B.V. on behalf of KeAi Communications Co. Ltd. This is an open access article under the CC

BY-NC-ND license (<http://creativecommons.org/licenses/by-nc-nd/4.0/>).

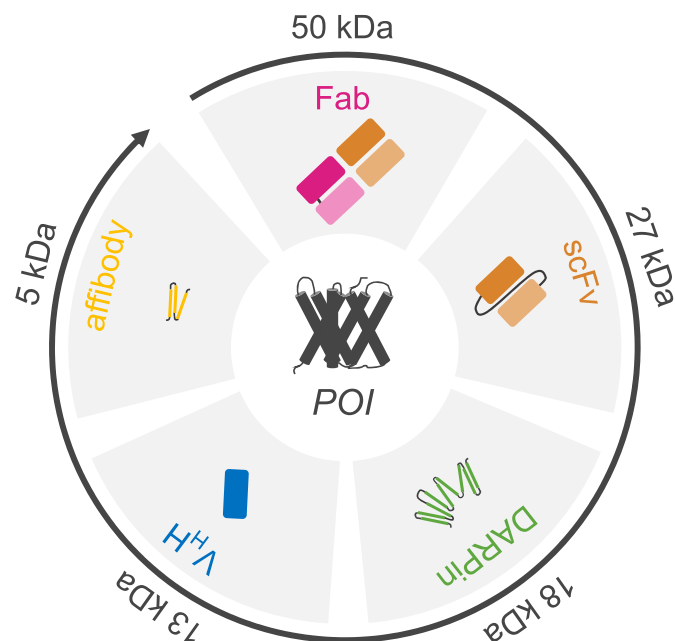


Fig. 1. Types of crystallization chaperones (CCs) for a protein of interest (POI).

techniques, phage libraries are inexpensive and have high throughput. They also enable antigen-antibody pairings under defined conditions. Once a F_{ab} is identified and sequenced, it can be expressed as a correctly

folded heterodimer in the periplasmic space of *E. coli* [22]. The so-called light and heavy chain subunits of the F_{ab} are independently expressed and secreted into the periplasm, where inter-subunit dimerization and disulfide bond formation occurs. While unoptimized protein titers are often low, several efforts aimed at improving F_{ab} expression levels have proved successful [23–25].

2.1. Examples of F_{ab} -POI complexes

Numerous F_{ab} -POI complexes have been structurally characterized to date. Through the following examples, we highlight the advantages of using a F_{ab} as a CC compared to smaller alternatives. F_{ab} s appear to be especially effective at enhancing crystallization by selecting and stabilizing a specific conformation of the POI. While a common apprehension to utilizing F_{ab} s is that they induce a non-native conformation, the prevalence of an energetically unfavorable conformer is inherently low. As such, the F_{ab} simply selects a conformation that already exists under the screening conditions. This is especially attractive for large protein complexes, such as PKs and membrane channels, that dynamically undergo significant conformational changes during their catalytic cycles. Screening large F_{ab} libraries against a POI under a range of conditions (e.g., presence or absence of substrate, high or low salt concentrations) has the potential to reveal distinct conformations. A historically prominent example of a F_{ab} stabilizing a protein conformation is that of the KcsA potassium ion channel, whose closed conformation was elucidated with a F_{ab} as a CC [26]. As of 1998 a crystal structure (3.2 Å) of the C-terminally truncated version of this ion channel had been solved (PDB ID 1BL8) [27]. However, a higher

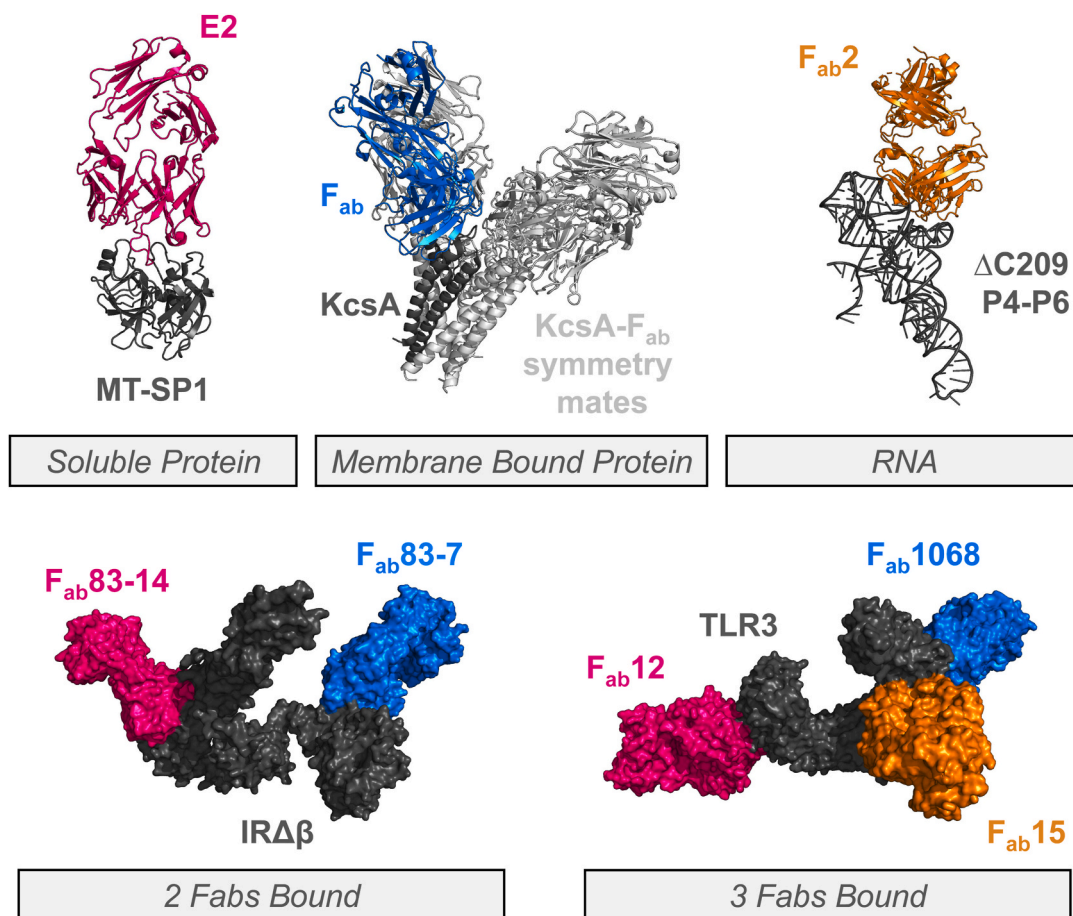


Fig. 2. Examples of structurally characterized F_{ab} -bound proteins. Broad application of F_{ab} s demonstrated: soluble (MT-SP1-E2; PDB ID 3BN9) [12] and membrane bound proteins (KcsA- F_{ab} ; PDB ID 1K4C) [13] and RNA (Δ C209 P4-P6- F_{ab2} ; PDB ID 2R8S) [14]. Use of multiple F_{ab} s bound to one target protein. IR $\Delta\beta$ - $F_{ab83-14}$ - F_{ab83-7} ; PDB ID 4ZXB (left) [15]. TLR3- F_{ab1068} - F_{ab12} - F_{ab15} ; PDB ID 3ULV (right) [18]. In all cases: POI (gray); F_{ab} (pink, orange, or blue).

resolution structure was required to reveal the specific location of ions within the channel. In 2001, a F_{ab} specific for the N-terminal tetrameric KcsA was deployed to improve resolution. The resulting structure [13] was solved at a high resolution (2.0 Å) in part due to protein contacts between neighboring F_{abs} (PDB ID 1K4C, Fig. 2). Despite this enhanced resolution, crystallization of the full-length protein remained elusive, presumably due to the inherent flexibility of the C-terminus that projected into the cytoplasm. Therefore, a C-terminal-specific F_{ab} was identified and utilized to obtain crystals. The structure of the full-length KcsA- F_{ab} (PDB ID 3EFF) [26], alongside an independent C-terminal-POI/ F_{ab} complex, was solved. The KcsA models could be overlaid with minimal differences, thus providing additional support (along with activity assays) that the F_{abs} did not induce “unnatural” structural changes.

In two other circumstances, the larger size of F_{abs} proved to be advantageous relative to smaller CCs (scFv, V_{HH}) that lacked multiple complementary determining regions (CDRs). The larger number of interacting residues offered the potential to mask more hydrophobic or flexible side chains that hindered crystallization while also providing an opportunity to optimize binding properties. In the case of ubiquitin, the linkage site (K63 versus K48) was known to influence the fate of the poly-ubiquitinated protein [28]. To understand the structural basis for these differences, researchers sought to identify K48- and K63-specific F_{abs} . From an initial library screen, Apu2.07 specifically bound the K48-linked di-ubiquitin ($K_d \sim 1$ nM). The K63-linked di-ubiquitin POI was recognized by Apu2.16 ($K_d \sim 90$ nM), although this F_{ab} was non-specific ($K_d \sim 40$ μ M for K48-linked di-ubiquitin). Following a round of affinity maturation, four clones were obtained with 10-fold enhanced binding for the K63-conjugated POI and no recognition capacity for the K48 adduct. Mutations in both the light and heavy chain CDRs had led to increased F_{ab} specificity.

In yet another example, an inhibitory scFv for the MT-SP1 protease was identified, however, Farady et al. [12] were unable to crystallize the complex. When the scFv was converted into a F_{ab} , crystals were readily

obtained (Fig. 2). The ability to obtain F_{ab} -MT-SP1 but not scFv-MT-SP1 crystals highlights the importance of the size of F_{abs} , which could lead to enhanced crystal contacts in the lattice.

Perhaps most interestingly, F_{abs} are not limited to single use for a POI. The ability to simultaneously bind two or even three distinct F_{abs} to the same target molecule (Fig. 2) highlights the versatility of these tools. In the case of the toll-like receptor TLR3, three F_{abs} were essential for crystallization [18]. The authors utilized several common techniques in an effort to obtain high-quality crystals. However, no crystals were obtained until three neutral F_{abs} were simultaneously bound to TLR3. These combined examples illustrate the broad usage of F_{abs} and, in many cases, how their use “saved the day”.

2.2. High-throughput methods for F_{ab} identification

F_{abs} have shown great promise as CCs however, due to their relatively low yield, it would be advantageous to determine their effect on crystallization before large scale production. Differential scanning fluorimetry (DSF) allows protein scientists to assess many F_{ab} CCs in a relatively high-throughput manner [29,30]. DSF only requires a quantitative PCR instrument to assess sample homogeneity, stability, and relative hydrophobic surface percentage. In DSF, a fluorescent dye recognizes the hydrophobic residues of a protein, which are exposed as a protein unfolds at higher temperatures (Fig. 3). Therefore, a comparison of DSF traces in the presence and absence of a F_{ab} can lead to the identification of a CC that enhances the stability (higher T_m) or surface properties (masked hydrophobic residues) of a POI. DSF paired with phage display selection of F_{abs} offers a powerful, high-throughput workflow to enhance crystallography efforts.

3. Polyketide synthases (PKSs)

A good test of one’s understanding of an enzyme’s structure-mechanism relationships is the ability to engineer the enzyme to

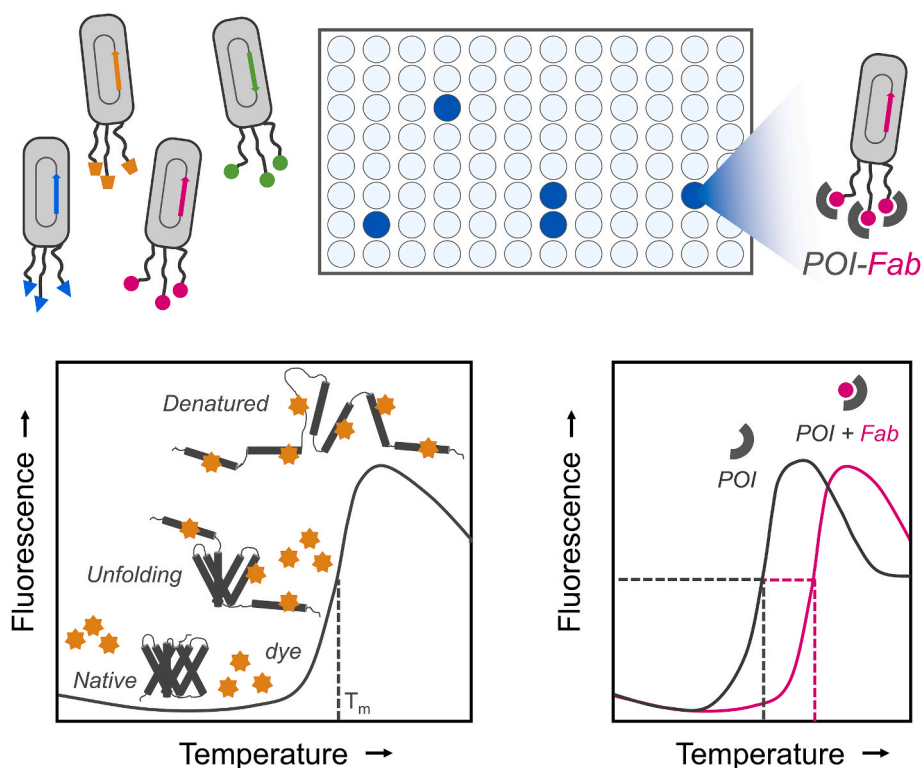


Fig. 3. High throughput methodology for determining advantageous F_{abs} for crystallography. Phage display libraries of F_{abs} are screened (ELISA) for potential binders to protein target (top), followed by DSF analysis of how the F_{ab} alters the POI’s physical properties (bottom).

exhibit a new property. Through a deeper understanding of active site structures, several enzymes have been engineered [31–33]; however, assembly-line PKSs have been relatively resistant to improvement via engineering [34–39]. These PKSs are large multifunctional and modular enzymes that are responsible for the biosynthesis of many medically relevant compounds. Their ability to catalyze stereospecific biosynthesis is especially striking. Minimally, a catalytic module of an assembly-line PKS is composed of three domains – ketosynthase (KS), acyltransferase (AT), and acyl carrier protein (ACP) [40]. Additional reducing domains – ketoreductase (KR), dehydratase (DH), enoyl reductase (ER) – establish the degree of reduction for each acyl unit (Fig. 4). The co-linear biosynthetic mechanisms of assembly-line PKSs [41,42] has inspired researchers to “mix-and-match” domains and modules to make novel natural products. Unfortunately, in most cases, the yields of these new products are often very low. It is generally believed that improvements in the catalytic activities of these hybrid enzymes would depend on an improved understanding of critical protein-protein and protein-substrate interfaces and interactions. Several PKS domains and multi-domain constructs have been structurally characterized at atomic resolution [43–53]. While these structures have undoubtedly provided insight into enzyme function, visualization of intact PKS modules is needed to understand the overall arrangement and cooperative functions of these assembly lines.

3.1. Relevance of F_{ab} s

Due to their inherent flexibility and large size, intact PKS modules have been resistant to structural characterization. Until recently, our understanding of PKS modules relied heavily on comparisons to the evolutionarily and functionally related vertebrate fatty acid synthases (FASs) [54]. The 4.5 Å structure (PDB ID 2CF2) of the porcine FAS [55, 56] was remarkably similar to the higher resolution structures of the KS-AT didomains of module 5 (PDB ID 2HG4) [49] and module 3 (PDB ID 2QO3) [51] of the 6-deoxyerythronolide B synthase (DEBS) as well as an analogous fragment from the curacin synthase [53] (PDB ID 4MZ0). In all cases the homodimeric protein assemblies had a dimeric ketosynthase (KS) interface flanked by acyltransferase (AT) domains on

either side (Fig. 5); this model has come to be referred to as the “extended” model of a PKS. More recent studies of the iterative lovastatin synthase LovB (Cryo-EM) [57] and DEBS module 2 (small-angle X-ray scattering, *i.e.*, SAXS) [58] support this “extended” architecture. However, a markedly distinct “arched” model (Cryo-EM) has been proposed for module 5 of the pikromycin PKS (PikAIII) [59,60].

In an effort to reconcile these differences while enhancing particle quality of these flexible megaenzymes, two efforts have recently leveraged the use of a F_{ab} , 1B2. 1B2 was identified from a phage-display library panned against DEBS module 3 [52] and was found to bind the N-terminal docking domain (DD) of this homodimeric protein. The crystal structure of 1B2 complexed with DD(3)-KS₃-AT₃ (PDB ID 6C9U) agreed with the previously reported “extended” conformations of KS-AT fragments. Because 1B2 did not inhibit the core catalytic activities of the module, it supported the hypothesis that the “extended” conformation is preserved throughout the catalytic cycle. Two recent Cryo-EM studies further underscore this hypothesis, both studies leveraged 1B2 and found the F_{ab} to be crucial in their analysis [61,62]. The Lasalocid A PKS module (Lsd14) was determined at 2.4 Å (X-ray) and 3.1 Å (Cryo-EM) resolutions, respectively. Meanwhile DEBS module 1 was resolved to 3.2–4.3 Å via Cryo-EM. Notably, both studies revealed asymmetric architectures of PKS modules, a feature that may have been overlooked in the solution of the PikAIII structure due to symmetry constraints imposed during data processing. Ongoing efforts are focused on generalizing the utility of a 1B2/DD(3)-PKS_{*i*} (where PKS_{*i*} represents any PKS module) model for cryo-EM analysis of PKS modules.

3.2. Future use of F_{ab} s

Although 1B2 has proven versatile for evaluating an entire PKS module, additional screening of multiple PKS modules against F_{ab} libraries is warranted. Identification of neutral F_{ab} s that bind different PKS epitopes could help resolve portions of Cryo-EM models that remain elusive. One portion of the PKS that remains especially difficult to model is the flexible TE domain [61]. The structure of a F_{ab} that recognizes the DEBS TE (3A6, PDB ID 6MLK) has been reported; this can be considered a neutral F_{ab} because the TE maintains its catalytic activity as part of the

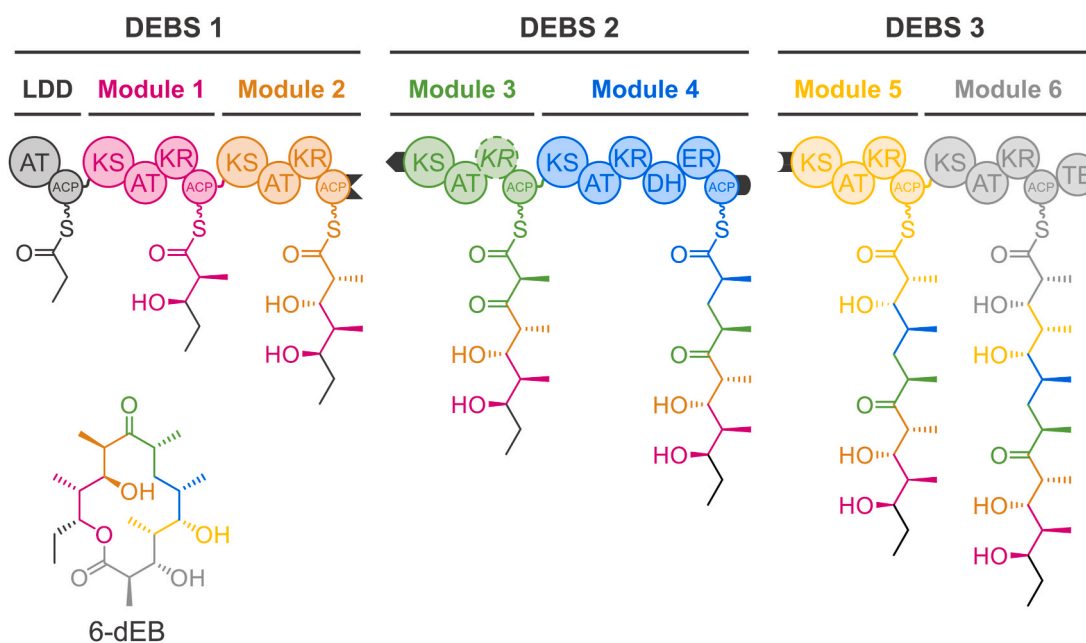


Fig. 4. Biosynthesis of 6-deoxyerythronolide B (6-dEB) by the 6-deoxyerythronolide B synthase (DEBS). DEBS is comprised of three large proteins, DEBS1, DEBS2 and DEBS3, each harboring two elongation modules. Each module performs one round of elongation and modification on the growing chain before translocating it to the next module. KS, ketosynthase; AT, acyltransferase; KR, ketoreductase; ACP, acyl carrier protein; DH, dehydratase; ER, enoyl reductase; TE, thioesterase. N- and C-terminal docking domains are shown in dark gray. KR₃ is inactive.

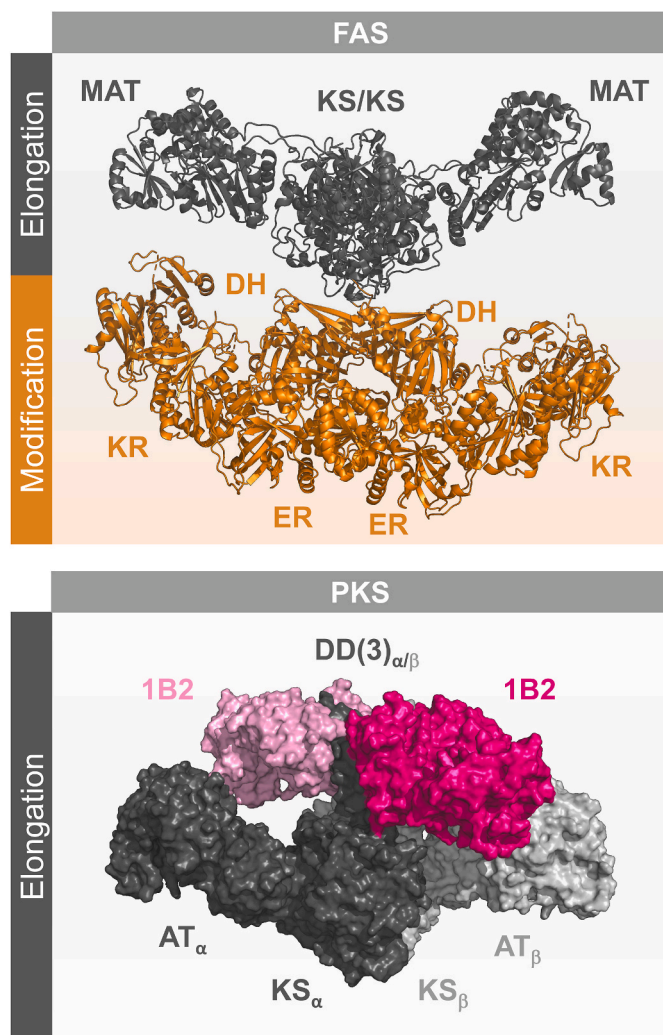


Fig. 5. Porcine mFAS (PDB ID 2VZ8) (top), “extended” architecture with dimeric KS/KS interface flanked by MAT domains on either end composing the elongation portion of the enzyme (gray). DH, ER, and KR domains outlined below in modification region (orange). DEBS DD(3)-KS₃-AT₃ (gray) bound to 1B2 (F_{ab}, pink) (bottom). α , β represent the two subunits of the homodimer.

complex [61,63]. As previously reported (Fig. 2), multiple non-competitive F_{abs} can enhance crystallization of a POI. Therefore, if 3A6 can be used in combination with 1B2, an enhanced PKS Cryo-EM model could be attained. Current models suggest 1B2 and 3A6 would bind “opposite ends” of the megasynthase, making this proposal reasonable for resolving the TE domain tethered to the module.

In contrast to 1B2 and 3A6, F_{abs} that inhibit specific reactions catalyzed by assembly-line PKSs are also likely to be useful. Two Fabs that bind the KR domain of Module 1 of DEBS have been reported (PDB ID 6WH9 and 6W7S) [64]; one of them (1D10) inhibits NADPH-dependent reduction of the growing polyketide chain. The ability to identify an inhibitory F_{ab} that changes the rate-limiting step in PKS turnover has the capacity to enhance our understanding of how the corresponding domain operates.

4. Concluding remarks

Crystallization of assembly-line PKSs is crucial for both fundamental understanding and our future ability to engineer new functions. Although traditional optimization techniques (cofactors, additives, etc.) are useful, they are limited for particularly challenging protein targets. Therefore, CCs have been employed in a broad range of applications to

enhance X-ray and Cryo-EM studies. We have focused on the use of F_{abs} as versatile CCs for PKSs. Their ability to stabilize specific conformations is particularly advantageous for highly flexible megasynthases which undergo large conformational changes during a catalytic cycle. This stabilizing effect has been recently exploited in two complementary Cryo-EM studies of PKS modules. In the future the use of multiple neutral F_{abs} that bind increasingly larger complexes may be helpful. The use of inhibitory F_{abs} to understand the catalytic chemistry of PKSs is also feasible and informative.

Declaration of competing interest

None.

CRediT authorship contribution statement

Katarina M. Guzman: Writing – wrote original draft, developed figures, and edited. **Chaitan Khosla:** Writing – reviewed and edited.

Acknowledgment

NIH grant R35 GM141799 (to C.K.). Stanford Graduate Fellowship (SGF) Award (to K.M.G.).

References

- [1] Koide S. Engineering of recombinant crystallization chaperones. *Curr Opin Struct Biol* 2009;19(4):449–57. <https://doi.org/10.1016/j.sbi.2009.04.008>.
- [2] Air GM, Webster RG, Colman PM, Laver WG. Distribution of sequence differences in influenza N9 neuraminidase of tern and whale viruses and crystallization of the whale neuraminidase complexed with antibodies. *Virology* 1987;160(2):346–54. [https://doi.org/10.1016/0042-6822\(87\)90005-5](https://doi.org/10.1016/0042-6822(87)90005-5).
- [3] Ostermeier C, Iwata S, Ludwig B, Michel H. Fv fragment-mediated crystallization of the membrane protein bacterial cytochrome c oxidase. *Nat Struct Biol* 1995;2(10):842–6. <https://doi.org/10.1038/nsb1095-842>.
- [4] Hamers-Casterman C, Atarhouch T, Muyldermans S, Robinson G, Hamers C, Songa EB, Bendahman N, Hamers R. Naturally occurring antibodies devoid of light chains. *Nature* 1993;363(6428):446–8. <https://doi.org/10.1038/363446a0>.
- [5] Barthelemy PA, Raab H, Appleton BA, Bond CJ, Wu P, Wiesmann C, Sidhu SS. Comprehensive analysis of the factors contributing to the stability and solubility of autonomous human VH domains. *J Biol Chem* 2008;283(6):3639–54. <https://doi.org/10.1074/jbc.M708536200>.
- [6] Tereshko V, Uysal S, Koide A, Margalef K, Koide S, Kossiakoff AA. Toward chaperone-assisted crystallography: protein engineering enhancement of crystal packing and X-ray phasing capabilities of a camelid single-domain antibody (VHH) scaffold. *Protein Sci* 2008;17(7):1175–87. <https://doi.org/10.1110/ps.034892.108>.
- [7] Rasmussen SG, Choi HJ, Fung JJ, Pardon E, Casarosa P, Chae PS, Devree BT, Rosenbaum DM, Thian FS, Kobilka TS, Schnapp A, Konetzki I, Sunahara RK, Gellman SH, Pautsch A, Steyaert J, Weis WI, Kobilka BK. Structure of a nanobody-stabilized active state of the $\beta(2)$ adrenoceptor. *Nature* 2011;469(7329):175–80. <https://doi.org/10.1038/nature09648>.
- [8] Eigenbrot C, Ultsch M, Dubnovitsky A, Abrahmsén L, Härd T. Structural basis for high-affinity HER2 receptor binding by an engineered protein. *Proc Natl Acad Sci U S A* 2010;107(34):15039–44. <https://doi.org/10.1073/pnas.1005025107>.
- [9] Sennhauser G, Grütter MG. Chaperone-assisted crystallography with DARPins. *Structure* 2008;16(10):1443–53. <https://doi.org/10.1016/j.str.2008.08.010>.
- [10] Huber T, Steiner D, Röthlisberger D, Plückthun A. In vitro selection and characterization of DARPins and Fab fragments for the co-crystallization of membrane proteins: the Na(+)-citrate symporter CitS as an example. *J Struct Biol* 2007;159(2):206–21. <https://doi.org/10.1016/j.jsb.2007.01.013>.
- [11] Veelsler D, Dreier B, Blangy S, Lichière J, Tremblay D, Moineau S, Spinelli S, Tegoni M, Plückthun A, Campanacci V, Cambillau C. Crystal structure and function of a DARPIn neutralizing inhibitor of lactococcal phage TP901-1: comparison of DARPIn and camelid VHH binding mode. *J Biol Chem* 2009;284(44):30718–26. <https://doi.org/10.1074/jbc.M109.037812>.
- [12] Farady CJ, Egea PF, Schneider EL, Darragh MR, Craik CS. Structure of an Fab-protease complex reveals a highly specific non-canonical mechanism of inhibition. *J Mol Biol* 2008;380(2):351–60. <https://doi.org/10.1016/j.jmb.2008.05.009>.
- [13] Zhou Y, Morais-Cabral JH, Kaufman A, MacKinnon R. Chemistry of ion coordination and hydration revealed by a K⁺ channel-Fab complex at 2.0 Å resolution. *Nature* 2001;414(6859):43–8. <https://doi.org/10.1038/35102009>.
- [14] Ye JD, Tereshko V, Frederiksen JK, Koide A, Fellouse FA, Sidhu SS, Koide S, Kossiakoff AA, Piccirilli JA. Synthetic antibodies for specific recognition and crystallization of structured RNA. *Proc Natl Acad Sci U S A* 2008;105(1):82–7. <https://doi.org/10.1073/pnas.0709082105>.
- [15] Croll TI, Smith BJ, Margetts MB, Whittaker J, Weiss MA, Ward CW, Lawrence MC. Higher-resolution structure of the human insulin receptor ectodomain: multi-

- modal inclusion of the insert domain. *Structure* 2016;24(3):469–76. <https://doi.org/10.1016/j.str.2015.12.014>.
- [16] Hunte C, Michel H. Crystallisation of membrane proteins mediated by antibody fragments. *Curr Opin Struct Biol* 2002;12(4):503–8. [https://doi.org/10.1016/S0959-440X\(02\)00354-8](https://doi.org/10.1016/S0959-440X(02)00354-8).
- [17] Griffin L, Lawson A. Antibody fragments as tools in crystallography. *Clin Exp Immunol* 2011;165(3):285–91. <https://doi.org/10.1111/j.1365-2249.2011.04427.x>.
- [18] Malia TJ, Obmolova G, Luo J, Teplyakov A, Sweet R, Gilliland GL. Crystallization of a challenging antigen-antibody complex: TLR3 ECD with three noncompeting Fabs. *Acta Crystallogr Sect F Struct Biol Cryst Commun* 2011;67(Pt 10):1290–5. <https://doi.org/10.1107/S1744309111030983>.
- [19] Derewenda ZS, Vekilov PG. Entropy and surface engineering in protein crystallization. *Acta Crystallogr D Biol Crystallogr* 2006;62(Pt 1):116–24. <https://doi.org/10.1107/S0907444905035237>.
- [20] Fellouse FA, Esaki K, Birtalan S, Raptis D, Cancasci VJ, Koide A, Jhurani P, Vasser M, Wiesmann C, Kossiakoff AA, Koide S, Sidhu SS. High-throughput generation of synthetic antibodies from highly functional minimalist phage-displayed libraries. *J Mol Biol* 2007;373(4):924–40. <https://doi.org/10.1016/j.jmb.2007.08.005>.
- [21] Hornsby M, Paduch M, Miersch S, Säaf A, Matsuguchi T, Lee B, Wypisniak K, Doak A, King D, Usatyuk S, Perry K, Lu V, Thomas W, Luke J, Goodman J, Hoey RJ, Lai D, Griffin C, Li Z, Vizeacoumar FJ, Dong D, Campbell E, Anderson S, Zhong N, Gräslund S, Koide S, Moffat J, Sidhu S, Kossiakoff A, Wells J. A high throughput platform for recombinant antibodies to folded proteins. *Mol Cell Proteomics* 2015;14(10):2833–47. <https://doi.org/10.1074/mcp.O115.052209>.
- [22] Skerra A. A general vector, pASK84, for cloning, bacterial production, and single-step purification of antibody Fab fragments. *Gene* 1994;141(1):79–84. [https://doi.org/10.1016/0378-1119\(94\)90131-7](https://doi.org/10.1016/0378-1119(94)90131-7).
- [23] Venturi M, Seifert C, Hunte C. High level production of functional antibody Fab fragments in an oxidizing bacterial cytoplasm. *J Mol Biol* 2002;315(1):1–8. <https://doi.org/10.1006/jmbi.2001.5221>.
- [24] Kulmala A, Huovinen T, Lamminmäki U. Effect of DNA sequence of Fab fragment on yield characteristics and cell growth of *E. coli*. *Sci Rep* 2017;7:3796. <https://doi.org/10.1038/s41598-017-03957-6>.
- [25] Bailey LJ, Sheehy KM, Dominik PK, Liang WG, Rui H, Clark M, Jaskolowski M, Kim Y, Deneka D, Tang WJ, Kossiakoff AA. Locking the elbow: improved antibody Fab fragments as chaperones for structure determination. *J Mol Biol* 2018;430(3):337–47. <https://doi.org/10.1016/j.jmb.2017.12.012>.
- [26] Uysal S, Vásquez V, Tereshko V, Esaki K, Fellouse F, Sidhu S, Koide S, Perozo E, Kossiakoff A. Crystal structure of full length KcsA in its closed conformation. *Proc Natl Acad Sci USA* 2009;106(16):6644–9. <https://doi.org/10.1073/pnas.0810663106>.
- [27] Doyle DA, Morais Cabral J, Pfuetzner RA, Kuo A, Gulbis JM, Cohen SL, Chait BT, MacKinnon R. The structure of the potassium channel: molecular basis of K⁺ conduction and selectivity. *Science* 1998;280(5360):69–77. <https://doi.org/10.1126/science.280.5360.69>.
- [28] Newton K, Matsumoto ML, Wertz IE, Kirkpatrick DS, Lill JR, Tan J, Dugger D, Gordon N, Sidhu SS, Fellouse FA, Komuves L, French DM, Ferrando RE, Lam C, Compaan D, Yu C, Bosanac I, Hymowitz SG, Kelley RF, Dixit VM. Ubiquitin chain editing revealed by polyubiquitin linkage-specific antibodies. *Cell* 2008;134(4):668–78. <https://doi.org/10.1016/j.cell.2008.07.039>.
- [29] Ericsson UB, Hallberg BM, Detitta GT, Dekker N, Nordlund P. Thermofluor-based high-throughput stability optimization of proteins for structural studies. *Anal Biochem* 2006;357(2):289–98. <https://doi.org/10.1016/j.ab.2006.07.027>.
- [30] Vivoli M, Novak HR, Littlechild JA, Harmer NJ. Determination of protein-ligand interactions using differential scanning fluorimetry. *JoVE* 2014;91:51809. <https://doi.org/10.3791/51809>.
- [31] Bozhüyüük KAJ, Fleischhacker F, Linck A, Wesche F, Tietze A, Niesert CP, Bode HB. De novo design and engineering of non-ribosomal peptide synthetases. *Nat Chem* 2018;10(3):275–81. <https://doi.org/10.1038/nchem.2890>.
- [32] Chen K, Arnold FH. Engineering new catalytic activities in enzymes. *Nat Catal* 2020;3:203–13. <https://doi.org/10.1038/s41929-019-0385-5>.
- [33] Thorson JS, Barton WA, Hoffmeister D, Albermann C, Nikolov DB. Structure-based enzyme engineering and its impact on in vitro glycorandomization. *Chembiochem* 2003;5:16–25. <https://doi.org/10.1002/cbic.200300620>.
- [34] Zargar A, Lal R, Valencia L, Wang J, Backman TWH, Cruz-Morales P, Kothari A, Werts M, Wong AR, Bailey CB, Loubat A, Liu YZ, Chen Y, Chang S, Benites VT, Hernandez AC, Barajas JF, Thompson MG, Barcelos C, Anayah R, Martin HG, Mukhopadhyay A, Petzold CJ, Baidoo EEK, Katz L, Keasling JD. Chemoinformatic-guided engineering of polyketide synthases. *J Am Chem Soc* 2020;142(22):9896–901. <https://doi.org/10.1021/jacs.0c02549>.
- [35] Klaus M, Grninger M. Engineering strategies for rational polyketide synthase design. *Nat Prod Rep* 2018;35(10):1070–81. <https://doi.org/10.1039/c8np00030a>.
- [36] Weissman KJ. Genetic engineering of modular PKSs: from combinatorial biosynthesis to synthetic biology. *Nat Prod Rep* 2016;33(2):203–30. <https://doi.org/10.1039/c5np00109a>.
- [37] Murphy AC, Hong H, Vance S, Broadhurst RW, Leadlay PF. Broadening substrate specificity of a chain-extending ketosynthase through a single active-site mutation. *Chem Commun (Camb)* 2016;52(54):8373–6. <https://doi.org/10.1039/c6cc03501a>.
- [38] Menzella HG, Reid R, Carney JR, Chandran SS, Reisinger SJ, Patel KG, Hopwood DA, Santi DV. Combinatorial polyketide biosynthesis by de novo design and rearrangement of modular polyketide synthase genes. *Nat Biotechnol* 2005;23(9):1171–6. <https://doi.org/10.1038/nbt1128>.
- [39] Menzella HG, Carney JR, Santi DV. Rational design and assembly of synthetic trimodular polyketide synthases. *Chem Biol* 2007;14(2):143–51. <https://doi.org/10.1016/j.chembiol.2006.12.002>.
- [40] Katz L. The DEBS paradigm for type I modular polyketide synthases and beyond. *Methods Enzymol* 2009;459:113–42. [https://doi.org/10.1016/S0076-6879\(09\)04606-0](https://doi.org/10.1016/S0076-6879(09)04606-0).
- [41] Lowry B, Li X, Robbins T, Cane DE, Khosla C. A turnstile mechanism for the controlled growth of biosynthetic intermediates on assembly line polyketide synthases. *ACS Cent Sci* 2016;2(1):14–20. <https://doi.org/10.1021/acscentsci.5b00321>.
- [42] Smith JL, Sherman DH. An enzyme assembly line. *Science* 2008;321(5894):1304–5. <https://doi.org/10.1126/science.1163785>.
- [43] Akey DL, Razelun JR, Tehrani S, Sherman DH, Gerwick WH, Smith JL. Crystal structures of dehydratase domains from the curacin polyketide biosynthetic pathway. *Structure* 2010;18(1):94–105. <https://doi.org/10.1016/j.str.2009.10.018>.
- [44] Keatinge-Clay AT. A tylosin ketoreductase reveals how chirality is determined in polyketides. *Chem Biol* 2007;14(8):898–908. <https://doi.org/10.1016/j.chembiol.2007.07.009>.
- [45] Zheng J, Taylor CA, Piasecki SK, Keatinge-Clay AT. Structural and functional analysis of A-type ketoreductases from the amphotericin modular polyketide synthase. *Structure* 2010;18(8):913–22. <https://doi.org/10.1016/j.str.2010.04.015>.
- [46] Zheng J, Gay DC, Demeler B, White MA, Keatinge-Clay AT. Divergence of multimodular polyketide synthases revealed by a didomain structure. *Nat Chem Biol* 2012;8(7):615–21. <https://doi.org/10.1038/nchembio.964>.
- [47] Moretto L, Heylen R, Holroyd N, Vance S, Broadhurst RW. Modular type I polyketide synthase acyl carrier protein domains share a common N-terminally extended fold. *Sci Rep* 2019;9:2325. <https://doi.org/10.1038/s41598-019-38747-9>.
- [48] Gay DC, Gay G, Axelrod AJ, Jenner M, Kohlhaas C, Kampa A, Oldham NJ, Piel J, Keatinge-Clay AT. A close look at a ketosynthase from a trans-acyltransferase modular polyketide synthase. *Structure* 2014;22(3):444–51. <https://doi.org/10.1016/j.str.2013.12.016>.
- [49] Tang Y, Kim CY, Mathews I, Cane DE, Khosla C. The 2.7-Ångstrom crystal structure of a 194-kDa homodimeric fragment of the 6-deoxyerythronolide B synthase. *Proc Natl Acad Sci U S A* 2006;103(30):11124–9. <https://doi.org/10.1073/pnas.0601924103>.
- [50] Broadhurst RW, Nietlispach D, Wheatcroft MP, Leadlay PF, Weissman KJ. The structure of docking domains in modular polyketide synthases. *Chem. Biol.* 2003;10:723–31. [https://doi.org/10.1016/S1074-5521\(03\)00156-X](https://doi.org/10.1016/S1074-5521(03)00156-X).
- [51] Tang Y, Chen AY, Kim CY, Cane DE, Khosla C. Structural and mechanistic analysis of protein interactions in module 3 of the 6-deoxyerythronolide B synthase. *Chem Biol* 2007;14(8):931–43. <https://doi.org/10.1016/j.chembiol.2007.07.012>.
- [52] Li X, Sevillano N, La Greca F, Deis L, Liu YC, Deller M, Mathews I, Matsui T, Cane D, Craik C, Khosla C. Structure-function analysis of the extended conformation of a polyketide synthase module. *J Am Chem Soc* 2018;140(21):6518–21. <https://doi.org/10.1021/jacs.8b02100>.
- [53] Whicher JR, Smaga SS, Hansen DA, Brown WC, Gerwick WH, Sherman DH, Smith JL. Cyanobacterial polyketide synthase docking domains: a tool for engineering natural product biosynthesis. *Chem Biol* 2013;20(11):1340–51. <https://doi.org/10.1016/j.chembiol.2013.09.015>.
- [54] Smith S, Tsai SC. The type I fatty acid and polyketide synthases: a tale of two megasynthases. *Nat Prod Rep* 2007;24:1041–72. <https://doi.org/10.1039/B603600G>.
- [55] Maier T, Jenni S, Ban N. Architecture of mammalian fatty acid synthase at 4.5 Å resolution. *Science* 2006;311(5765):1258–62. <https://doi.org/10.1126/science.1123248>.
- [56] Maier T, Leibundgut M, Ban N. The crystal structure of a mammalian fatty acid synthase. *Science* 2008;321(5894):1315–22. <https://doi.org/10.1126/science.1161269>.
- [57] Wang J, Liang J, Chen L, Zhang W, Kong L, Peng C, Su C, Tang Y, Deng Z, Wang Z. Structural basis for the biosynthesis of lovastatin. *Nat Commun* 2021;12(1):867. <https://doi.org/10.1038/s41467-021-21174-8>.
- [58] Klaus M, Rossini E, Linden A, Pattharankar KS, Zeug M, Ignatova Z, Urlaub H, Khosla C, Köfinger J, Hummer G, Grninger M. Solution structure and conformational flexibility of a polyketide synthase module. *J Am Chem Soc* 2021. <https://doi.org/10.1021/jacsau.1c00043>. Article.
- [59] Dutta S, Whicher JR, Hansen DA, Hale WA, Chemler JA, Congdon GR, Narayan AR, Håkansson K, Sherman DH, Smith JL, Skiniotis G. Structure of a modular polyketide synthase. *Nature* 2014;510(7506):512–7. <https://doi.org/10.1038/nature13423>.
- [60] Whicher JR, Dutta S, Hansen DA, Hale WA, Chemler JA, Dosey AM, Narayan AR, Håkansson K, Sherman DH, Smith JL, Skiniotis G. Structural rearrangements of a polyketide synthase module during its catalytic cycle. *Nature* 2014;510(7506):560–4. <https://doi.org/10.1038/nature13409>.
- [61] Cogan D, Zhang K, Li X, Li S, Pintilie GD, Roh SH, et al. Mapping the catalytic conformations of an assembly-line polyketide synthase module. *Science* 2021;374(6568):729–34. <https://doi.org/10.1126/science.abi8358>.

- [62] Bagde S, Mathews I, Fromme C, Kim CY. Asymmetric architecture of type I modular polyketide synthase revealed by X-ray and cryo-EM. *Science* 2021;374(6568):723–9. <https://doi.org/10.1126/science.abi8532>.
- [63] Li X, Sevillano N, La Greca F, Hsu J, Mathews II, Matsui T, Craik CS, Khosla C. Discovery and characterization of a thioesterase-specific monoclonal antibody that recognizes the 6-deoxyerythronolide B synthase. *Biochemistry* 2018;57(43):6201–8. <https://doi.org/10.1021/acs.biochem.8b00886>.
- [64] Cogan D, Li X, Sevillano N, Mathews I, Matsui T, Craik C, Khosla C. Antibody probes of module 1 of the 6-deoxyerythronolide B synthase reveal an extended conformation during ketoreduction. *J Am Chem Soc* 2020;142:14933–9. <https://doi.org/10.1021/jacs.0c05133>.